



Copper Sulfide Nanowire Growth and Characterization

Chairote Piyakulworawat, Mahidol University, Thailand

September 8, 2015

Abstract

One-dimensional (1D) nanostructures (nanowires, nanorods, nanotubes, etc.) have become a central topic of research in past decades. Painstaking preparation has been done on nanostructured copper chalcogenides. It is well established that copper sulfide possesses the so-called superionic property of which a critical temperature is higher than 100°. Recent work in nanoscale superionics has shown that the transition temperature is reduced at small sizes and those polymer-surface treatments enable stabilization of the superionic phase to room temperature. We have synthesized Cu_2S nanowires using template free electrochemical technique and tried to characterize using conventional techniques.

Contents

1	Introduction	3
2	Theoretical concepts	3
2.1	Electrochemical cell	4
2.2	Potentiostat	5
2.3	Growth mechanism	9
2.4	Scanning electron microscope	11
2.5	Energy-dispersive x-ray spectroscopy	12
2.6	X-ray diffraction	13
3	Experimental detail	13
3.1	Synthesis	14
3.2	Characterization	15
4	Results and discussion	15
4.1	Pulse electrodeposition	15
4.2	Morphology	15
4.3	Elemental components	16
4.4	Structure of nanowire	17

1 Introduction

One-dimensional nanostructures, e.g., nanowire, nanorod, nanotube, have become a central topic of research in modern science. This is because of their unique application in mesoscopic physics and fabrication of nanoscale devices. General fabrication techniques, applications for, and characterization of 1D nanostructures have been studied extensively. Recent efforts have been directed toward the preparation of nanostructured copper chalcogenides. Copper sulfides (in different stoichiometries) possess unique optical and electrical properties, and therefore widely used in solar cells as optical filters and also as super ionic materials.

Superionic conductors are solids that exhibit a critical temperature close to ambient, increasing the technological applicability of this unique solid-liquid hybrid behavior. For example, copper (I) sulfide exhibits superionicity above 103 °C, where the monoclinic sulfur lattice expands into largely vacant hexagonal structure; the copper ions, for which there are many more sites than ions, abandon their fixed low-temperature positions and move freely among the many possible sites in hexagonal sulfur lattice, displaying the characteristic high ionic conductivity of superionic phases.

Recent work in nanoscale superionics has shown that the transition temperature is reduced at small sizes and those polymer-surface treatments enable stabilization of the superionic phase to room temperature. We have synthesized Cu_2S nanowire using template-free electrochemical technique and tried to characterize using conventional characterization techniques.

2 Theoretical concepts

When the size of the materials is down to the nanoscale, the temperatures of fusion and of order-disorder phase transitions can be lowered as the proportion of surface atoms increases, resulting in an increase of surface energy. Stabilization of high-temperature phases at lower temperatures or melting-point depressions have been reported in metal, metal oxide, and semiconductor nanoparticles or thin films. Similarly, there are reports of lowering the phase transition temperature, T_c , in AgI nanoplates, and in AgI nanowires. Cu_2S is a superionic solid whose bulk superionic transition temperature is 103°C. In the first part of the project we have synthesized Cu_2S nanowires, and in the second part we have characterized it. The technique of electrochemical deposition is used to make such nanowire. To do electrochemical deposition, a conventional three-electrode electrochemical cell is coupled with a potentiostat to perform the task. After obtaining the sample, optical and scanning electron microscopes are employed to study the morphology. The techniques of energy-dispersive X-ray spectroscopy and X-ray diffraction are, then, performed to study elemental composition and structure, respectively.

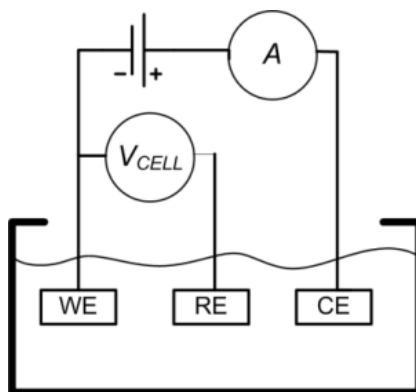


Figure 1: A schematic of the conventional three-electrode electrolytic cell. Here, WE, RE, CE stand for working, reference, and counter electrodes. A and V are ammeter and voltmeter, respectively.

2.1 Electrochemical cell

Nowadays, there are a large number of techniques which are capable of growing nanowire. In the present work, Cu_2S nanowire is synthesized by a technique of electrochemical method. A square-pulsed voltage is applied on the working electrode of the conventional three-electrode electrochemical cell. The simplest configuration of this kind of electrode is depicted in Figure 1.

Working electrode

The working electrode is an electrode in an electrochemical cell on which, in our case, the deposition occurs. Since the working electrode is where the reduction or oxidation reaction goes on, it should be made of inert materials to prevent it from reaction with the solution. In the present work, platinum is employed to be the working electrode. That the working electrode is called cathodic or anodic depends upon whether the reaction is reduction or oxidation, respectively.

Reference electrode

The reference electrode is an electrode with highly stable and well-known electrode potential. Since, in practice, it is yet impossible to measure any electrode potential in isolation, the reference electrode is, then, used as a half cell of a whole cell to determine the potential of the other electrode. Namely, the electrode potential of the working electrode must be quoted with respect to the reference electrode.

In our case, a Ag/AgCl reference electrode is used. This electrode consists of a pure silver wire in a solution of KCl saturated with solid silver chloride. The potential of the electrode at $25\text{ }^\circ\text{C}$ is 0.197 V vs NHE.

Counter electrode

The counter electrode is an electrode which is used in a three-electrode electrochemical cell, and, along with the working electrode, it provides circuit on which a current is applied. It plays a role of anode when the working electrode is being cathode and vice versa. The potential of the counter electrode is usually not of interest, but rather adjusted so as to balance the reaction occurring at the working electrode. This allows us to measure the potential of the working electrode with respect to that of reference electrode without undermining its stability by passing current through it.

2.2 Potentiostat

In every electrochemical deposition, potential difference across working electrode and solution surrounding it is of crucial importance. Since the deposition merely occurs at certain value of potential difference between the two. Hence, controlling such a quantity is one significant part of our job. Not only is the potential difference controlled, but also measured to make sure that the working electrode is at the desired potential. An equipment whose default role is to control and measure a potential difference is called a potentiostat. Hence, by using a potentiostat in electrochemical cell, the potential difference between the working and reference electrodes is controlled and measured at all times.

The principal component of a modern potentiostat is the operational amplifier (op amp.) Figure 2 illustrates the symbol of the op amp in electric circuits. V_- and V_+ are inverting and non-inverting inputs, respectively. ΔV_S is defined as the voltage difference between

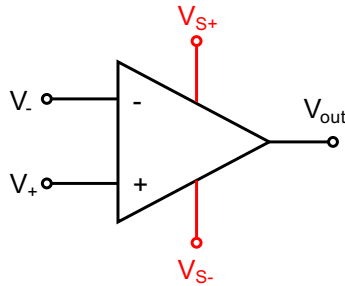


Figure 2: The symbol of the operational amplifier in electric circuits

non-inverting and inverting inputs.

$$\Delta V_S \equiv V_- - V_+. \quad (1)$$

The function of an op amp is to amplify the voltage difference between the two inputs, ΔV_S , by a factor of G which is called the open loop gain.

$$V_{\text{out}} \equiv -\Delta V_S \cdot G \quad (2)$$

For an ideal op amp, the open loop gain is infinitely large so that an infinitesimal input voltage difference ΔV_S can drive the output to infinity. Thus, if an op amp is included in any electric circuitry, the two inputs must be at the same value by design. The main building blocks in a potentiostat are voltage follower, current follower, and control amplifier, which are all based upon op amps.

Voltage follower

The voltage follower is based upon voltage feedback. In figure 3, a schematic picture of the voltage follower is shown. We can see that the inverting input is fed by output voltage V_{out} . Therefore, equation 1 gives $\Delta V_S = V_{out} - V_+$. Then, according to equation

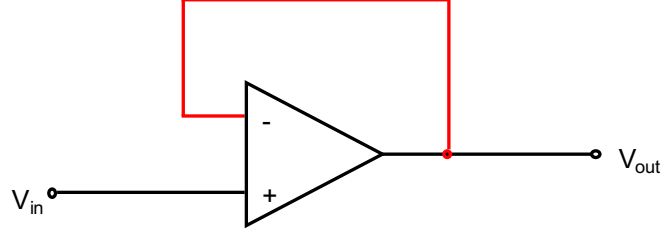


Figure 3: The symbol of the voltage follower

2, we have

$$V_{out} = -(V_{out} - V_+)G. \quad (3)$$

Solving this equation for V_+ yields

$$V_+ = V_{out} \left(1 + \frac{1}{G} \right). \quad (4)$$

From the fact that an op amp is designed to have an infinite open loop gain factor, equation 4, thus, reduces to $V_{out} = V_+$. That means the input impedance is infinity.

Current follower

The current follower is based upon current feedback. As shown in figure 4, V_+ is grounded, and the input current is fed by the output I_f . At point S, Kirchhoff's junction rule gives $I_{in} + I_f = 0$, or $I_f = -I_{in}$. According to Ohm's law, $I_f = (V_{out} - V_S)/R_f$. Hence,

$$I_{in} = - \left(\frac{V_{out} - V_S}{R_f} \right). \quad (5)$$

Since V_+ is grounded, $\Delta V_S = V_- \equiv V_S$. And equation (2) gives $V_{out} = -V_S \cdot G$, yielding $V_S = -V_{out}/G$. Hence,

$$I_{in} = - \left(\frac{V_{out} - V_{out}/G}{R_f} \right). \quad (6)$$

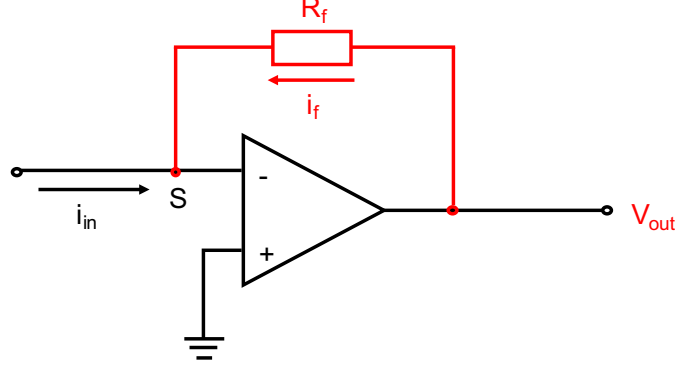


Figure 4: The symbol of the current follower

Solving this equation for V_{out} provides

$$V_{\text{out}} \left(1 + \frac{1}{G} \right) = -I_{\text{in}} R_f. \quad (7)$$

Because of the infinite open loop gain factor of the op amp, equation (7) reduces to $V_{\text{out}} = -I_{\text{in}} R_f$. That means that a current follower converts current to voltage and vice versa. This implies that the current is merely controlled by the voltage.

Control amplifier

The schematic picture of the control amplifier is displayed in figure 5. First of all, we have to find out what the value of the voltage at point S is by using the fact that non-inverting input voltage is grounded. So, $\Delta V_S = V_- - 0 = V_- \equiv V_S$. Then equation (2) provides $V_S = -V_{\text{out}}/G \rightarrow 0$ for an ideal op amp. That means point S is a virtual ground. Since the input impedance of an op amp is infinite, there can be no any input current. According to Ohm's law, we have $V_{\text{in}} - V_S = V_{\text{in}} = IR$ and $V_S - V_C = -V_C = IR$. Therefore, $V_C = -V_{\text{in}}$. And because $V_C = V_A$, hence

$$V_A = -V_{\text{in}}. \quad (8)$$

In addition, $V_A - 0 = I_0 R_2$ and $V_{\text{out}} - 0 = I_0 (R_1 + R_2)$. Thus,

$$V_{\text{out}} = - \left(\frac{R_1 + R_2}{R_2} \right) V_{\text{in}} \quad (9)$$

The output voltage V_A is set to $-V_{\text{in}}$ with respect to ground all the times.

Basic potentiostat

Now it is possible to use a control amplifier as a potentiostat as indicated in Figure 6. From this figure, it is seen that the potential of the working electrode with respect to the reference electrode is controlled and measured all the time. Yet, with this potentiostat

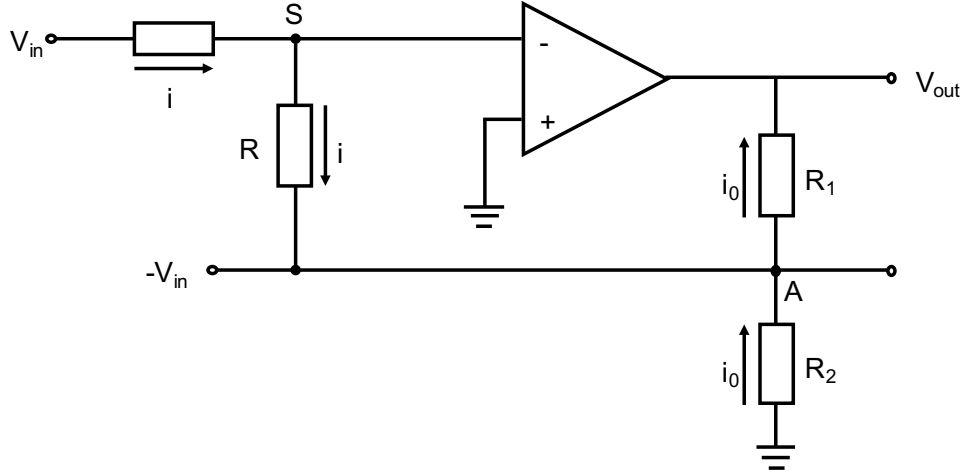


Figure 5: The symbol of the current follower

concept, we still encounter another issues. Since an op amp used in the control amplifier is a real op amp, then the open loop gain is not infinite. So, the reference electrode can pull out some current from the cell causing the potential to change. Therefore, it is a good idea to add a voltage follower right before the reference electrode to prevent current leakage from the cell. Moreover, the current follower is added to the working electrode so that we can measure the current flowing through this electrode. Eventually, the format of the basic potentiostat should look like in Figure 10.

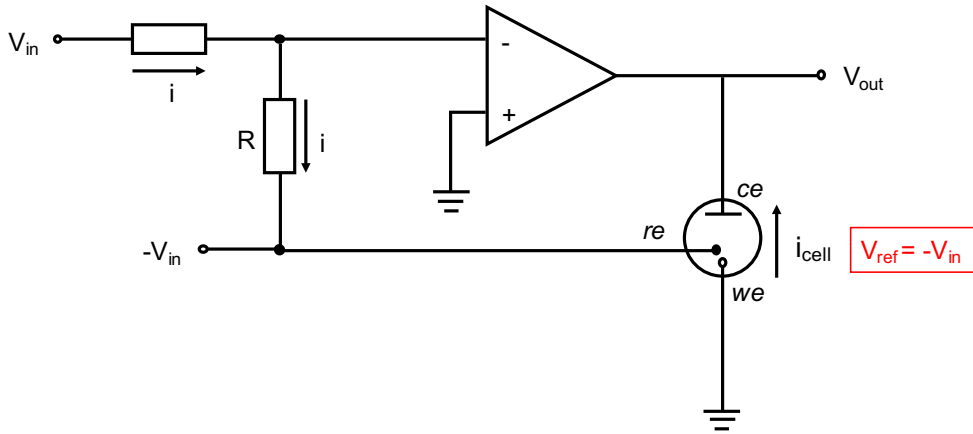


Figure 6: Schematic picture of the basic potentiostat

To perform electrochemical deposition, the potential difference between the working electrode and the solution surrounding it has to be remained constant. So, the reference electrode should be placed as close as possible to the working electrode so that it mea-

sures the potential of the solution, and, therefore, the potential difference is controlled at certain constant value.

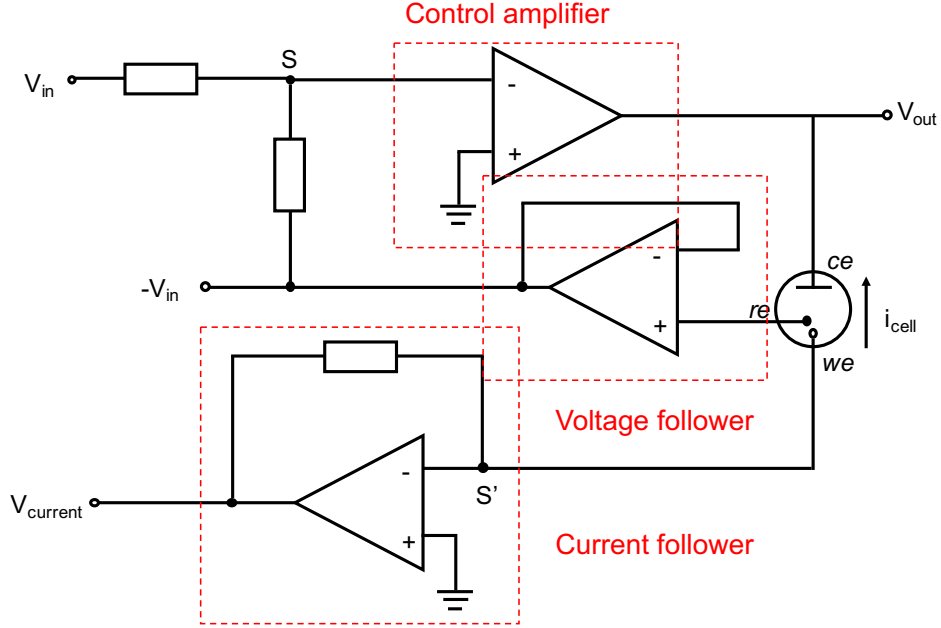
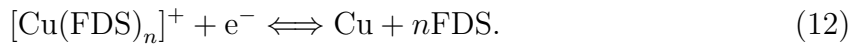
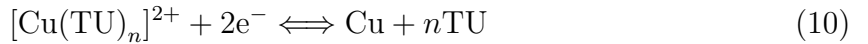


Figure 7: Schematic picture of the basic potentiostat

2.3 Growth mechanism

The growth mechanism was proposed earlier in a report [1]. The detail of the proposed growth mechanism is described below. In this experiment, every step has to be performed in quiescent conditions and low concentration of electrolyte. A square pulse of certain frequency and duty cycle is applied on the working electrode of an electrochemical cell. A cycle of the pulse consists of two parts: reverse voltage V_R of 0 V vs Ag/AgCl where the anodic current flows and forward voltage V_F of -0.9 V vs Ag/AgCl where the cathodic current flows.

In the cathodic portion of the cycle, copper ion complexes with TU and FDS are reduced and form copper nuclei on the platinum substrate according to reaction 10-12.



Simultaneously, TU is also reduced via reaction 13 to form sulfide.



Hence, in this portion of the cycle, copper atoms get deposited on the platinum substrate and the concentrations of S^{2-} , adsorbed sulfide, CN^- , and NH_4^+ increase around the plate. Then the voltage is increased to 0 V vs Ag/AgCl, anodic portion, and some deposited copper atoms get dissolved by free TU's and chloride ions. These copper ions are expected to form complexes with free TU, $CuTU$. Consequently, the concentration of TU decreases.

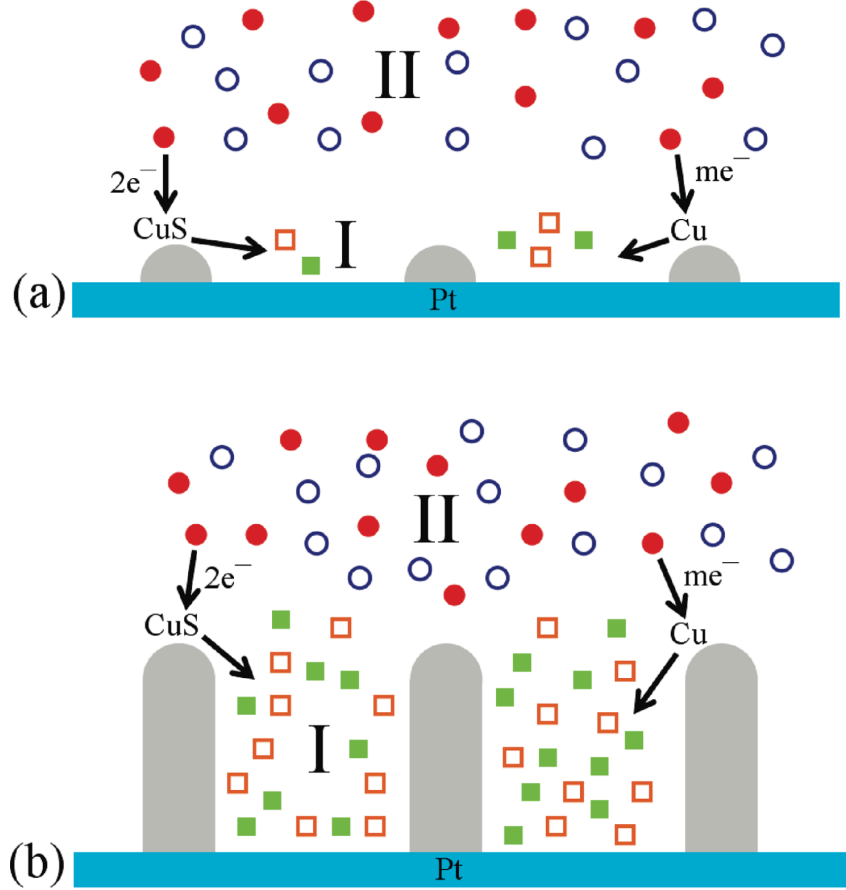
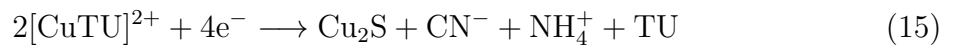


Figure 8: Proposed mechanism of nanowire growth

In the second cathodic cycle, copper sulfides are produced from $CuTU$ via reaction 14 and they deposit on the platinum substrate.



Not only is CuS produced in this cathodic cycle, but also Cu_2S via reaction 15.



Therefore, copper and copper sulfides deposition takes place during the pulsed voltage. Because the deposition is carried out with low concentration of electrolyte, the process rapidly exhausts copper ion complexes near the surface of the substrate. Moreover, CN^- and NH_4^+ , which are produced from reaction 13, 14, and 15, accumulate in region II causing this it to be depleted of electroactive copper ion complexes. These two facts, therefore, prohibit further nucleation on the platinum surface. Another copper ions must diffuse out of other region in the electrolyte and come to the tips, stronger electric field, of the deposited copper sulfides making the deposition to grow in one dimension. In summary, three things are produced during cathodic pulses: copper, CuS , and Cu_2S nanowire.

2.4 Scanning electron microscope

Scanning electron microscope or SEM is one type of electron microscope by which magnified surface topography of a specimen is produced. In an SEM, a beam of electrons is focused to a very fine line and scanned across the surface of a specimen. By this manner, SEMs produce many types of signals which are then detected by detectors inside the instrument. When an electron beam is incident on the surface, the beam can simply elastically scatter off the sample creating a signal which is also known as back-scattered electrons. The incident electrons can also knock off bounded electrons inside the atoms near the surface of the sample whereby two signals come out, the knocked off electrons itself, which is called secondary electrons, and x-ray photons generated by energy transition of electrons in higher levels to vacancies, i.e., empty levels, caused by secondary electrons. The current of secondary electrons varies as the beam scans across the specimen. Thus, this varying strength of the signal is used to construct the image. Moreover, the current also depends upon the angle at which the beam hits the surface, the image, hence, looks more three-dimensional than another types of microscopes.

The standard scanning electron microscope consists of the following components (Figure 9):

- **Electron gun:** This device produces electron beams to operate the instrument. The electron gun comes in two types, thermionic and field emission guns. For the former, typical kind, the filament is heated so that electrons are liberated and move toward the specimen. The latter, on the other hand, uses strong electric field to pull out electrons from the source.
- **Lenses:** These are magnetic fields capable of bending the beam's trajectory so that the beam gets focused and controlled to go where we want.
- **Sample chamber:** This is where a specimen is mounted. This chamber can also adjust the orientation of the specimen so that we do not have to remount it to get different images.

- Detectors: Since there are more than one process occurring after the beam hits the sample, there have to be more than one kind of detectors as well. The one which detects secondary electrons is called Everhart-Thornley, and this produces the best image of the specimen. Detectors for x-ray and back-scattered electrons can analyze the composition of samples.
- Vacuum chamber: Because the electron beams can get blocked by the air molecules, and ionized air molecules are capable of distorting the image, SEM must operate in vacuum chamber.

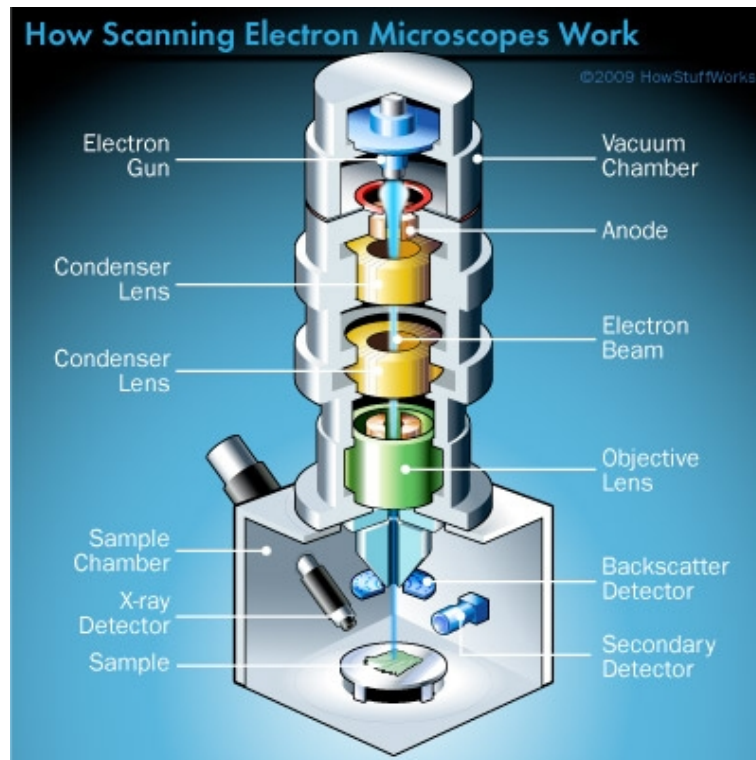


Figure 9: Various components of standard SEM

2.5 Energy-dispersive x-ray spectroscopy

Energy-dispersive x-ray spectroscopy (EDX) is an analytical technique which is used to determine atomic structure or chemical components of a specimen. By this manner, a specimen is bombarded by an incident beam of electrons. Typically, in the case of electrons, the incident energy ranges from 5 to 50 keV. And in this energy region, there are three processes taking place in this situation. First, the incident electrons simply scatter off the target atoms according to the Coulomb interaction. Secondly, they hit massive nuclei and stop moving resulting in production of photons of which the energy is derived

from that of the incident electron. In this second case, the emitted photons constitute a continuous spectrum, also known as Bremsstrahlung. Finally, if the incident energy is greater than that of ionization, electrons in internal levels can be knocked off resulting in electron hole formation. Because every system tries to establish the minimum energy, electrons in outer levels will, subsequently, fill the hole and radiate x-ray photons. According to the fact that each atom has a unique electronic structure, i.e., sets of energy levels are different for dissimilar elements, hence the x-ray spectrum is characteristic to each element. Therefore, this allows us to determine elemental components of a sample.

The emitted x-ray, both Bremsstrahlung and characteristic, can be detected by a detector. Although there exists two kinds of x-ray spectra, the characteristic one contains a set of sharp peaks of which the intensities are much higher than that of Bremsstrahlung. So Bremsstrahlung is considered as a background radiation and elemental constituents are specified by characteristic lines.

2.6 X-ray diffraction

To perform x-ray diffraction experiment, an x ray beam is incident on a specimen. The elastically scattered ray is, then, detected at a detector. Suppose that the incident and scattered wave vectors of an x ray beam are \mathbf{k} and \mathbf{k}' , respectively. The condition for constructive interference is

$$\mathbf{K} = \mathbf{k} - \mathbf{k}', \quad (16)$$

where \mathbf{K} represents reciprocal lattice vector which is specific for each structure. This condition for constructive interference is also known as von Laue condition. The position on the spectrum of detected scattered x ray is called the Bragg peak. The von Laue condition can also be represented by a geometry construction, the Ewald sphere. To construct the Ewald sphere, the origin of the incident wave vector is placed at one of the reciprocal lattice point. The Ewald sphere is a sphere in reciprocal space which is centered on the tip of wave vector \mathbf{k} . The lattice point on the surface of this sphere fulfil the von Laue condition, equation (16).

In the present work, a beam of monochromatic x ray is directed to the sample. A polycrystalline sample can be thought of as a lot of small crystallites whose orientation are random. That is equivalent to having a crystal simultaneously rotated in all direction. Therefore, the lattice points, which is now rotated around 360° in the plane, will form a sphere, which is called the powder sphere. Bragg peaks in this case are located where the powder sphere intersects the Ewald sphere with a fixed incident \mathbf{k} in three dimensions.

3 Experimental detail

The experiment can be divided into two main parts. The first part is synthesis and the other is characterization.

3.1 Synthesis

Electrochemical cell

A conventional three-electrode electrochemical cell is used in this nanowire deposition. For this electrochemical cell, a platinum plate is used as the working electrode, a sheet of graphite the counter electrode, and the reference electrode is of Ag/AgCl type. In order to control deposition to take place merely on one side of the platinum plate and not on the edges, the plate is covered by tape in such a way that there is only a small area left to be exposed to the solution. And the same thing is also done on the graphite counter electrode.

To prepare the electrolyte, $\text{CuSO}_4 \cdot 5\text{H}_2\text{O}$ and TU are used as copper and sulfur sources, respectively. 1.0 mM of $\text{CuSO}_4 \cdot 5\text{H}_2\text{O}$ and 4 mM of TU are prepared as followed. 0.250 g of $\text{CuSO}_4 \cdot 5\text{H}_2\text{O}$ and 0.304 g of TU are separately dissolved in certain amounts of deionized water. TU is dissolved by a manner of sonication. After the solutions turn clear, they are mixed together. The solution's volume is increased to 1 L by adding DI water and the pH is adjusted by adding certain amount of HCl. The amounts of HCl and pH in each experiment are indicated in Table 1.

Potentiostat

First of all, a potentiostat is built according to section 2.2. Figure 10 shows this poten-

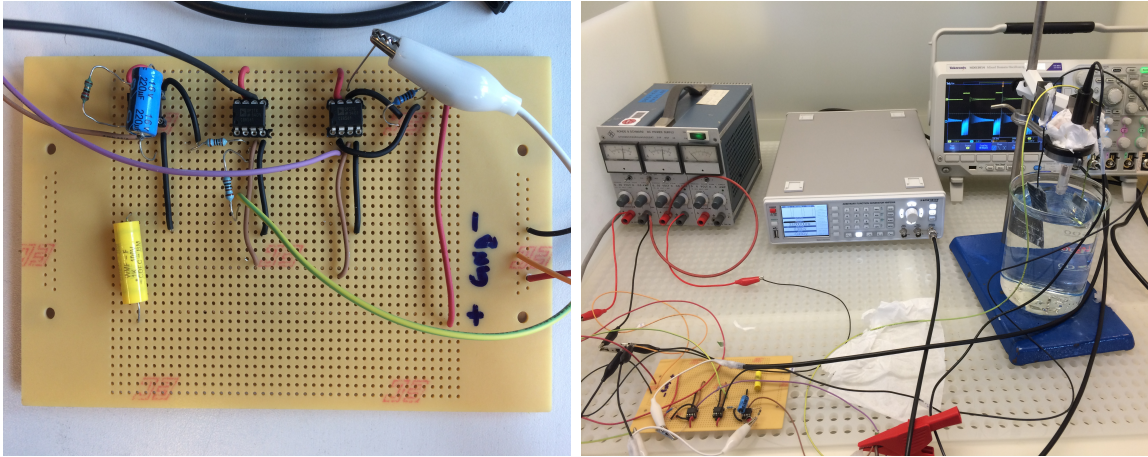


Figure 10: (Left) The potentiostat built according to section 2.2. (Right) The setup of all instrument

tiostat. In addition to the basic components shown in Figure 10, we have added two capacitors across the d.c. power supply and from the voltage follower output to the ground, in order to reduce noise which is high-frequency current. For this potentiostat, $R_1 = R_2 = 1 \text{ k}\Omega$, $R_3 = 100 \Omega$, $C_1 = 0.1 \mu\text{F}$, and $C_2 = 220 \mu\text{F}$.

Deposition

Before every deposition, the platinum working electrode is cleaned by propanol and the graphite counter electrode is replaced by a new one. A square-pulse alternating voltage is applied on the cell to do a deposition. The anodic current flows at reverse potential of 0.0 V vs Ag/AgCl, and the cathodic current flows at forward potential of -0.9 V vs Ag/AgCl. The duty cycle is set to 20%. The deposition time is approximately 30 minutes.

Table 1: The amount of HCl and pH

	HCl(mL)	pH
First	10	0.9
Second	5	1.2
Third	2	1.6

3.2 Characterization

For characterization of the deposits, three experiments are performed. In order to study the morphology of the deposit, the sample were investigated under the scanning electron microscope. Secondly, Energy-dispersive x-ray spectroscopy is performed to study the deposit's elemental contents. And, finally, the structure of the sample is examined by the x-ray diffraction technique.

4 Results and discussion

4.1 Pulse electrodeposition

To ensure that square-pulsed voltage is applied on the cell the potential difference between the working and reference electrodes is measured (yellow curve). This is illustrated in Figure 11. Voltage across the 100 Ω resistor in the current follower shows us the current in the cell (blue curve). Figure 12 illustrates the deposit on the platinum substrate. The material on the opaque white area in the center of the substrate is expected to be the nanowire.

4.2 Morphology

The sample is examined using optical and scanning electron microscopes. Figure 13 shows images seen under these microscopes. The objective lens of the optical microscope has magnifying power of 50 times. And the magnifying power of the scanning electron microscope is indicated in the figures. We have found that with the change of pH of the

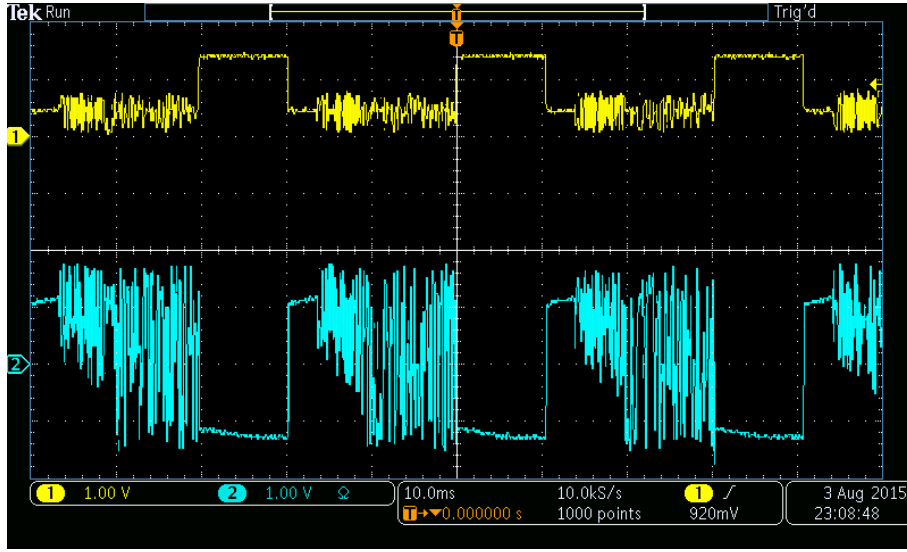


Figure 11: (Yellow) Potential difference between working and reference electrodes. (Blue) Output voltage of the current follower (the resistance of the current follower is 100Ω).

electrolyte the average diameter of grown nanowire changes. The variation of nanowire diameter with pH is presented in Table 2. For the measurement we have used SEM.

Table 2: The correlation between pH and diameter

	pH	diameter(nm)
First	0.9	500-550
Second	1.2	350-400
Third	1.6	70-80

4.3 Elemental components

In order to detect elements present in the nanowire, we have selected finite region of the nanowire and did the energy-dispersive x-ray spectroscopy presented in Figure 14. Then we did elemental mapping of the selected zone of the nanowire which is shown in Figure 15. The particular region on which the density is studied is shown in Figure 13(f). The energy of x-ray ranges from 0 to around 20 keV. According to the characteristic lines in the spectrum, the following elements have been detected:

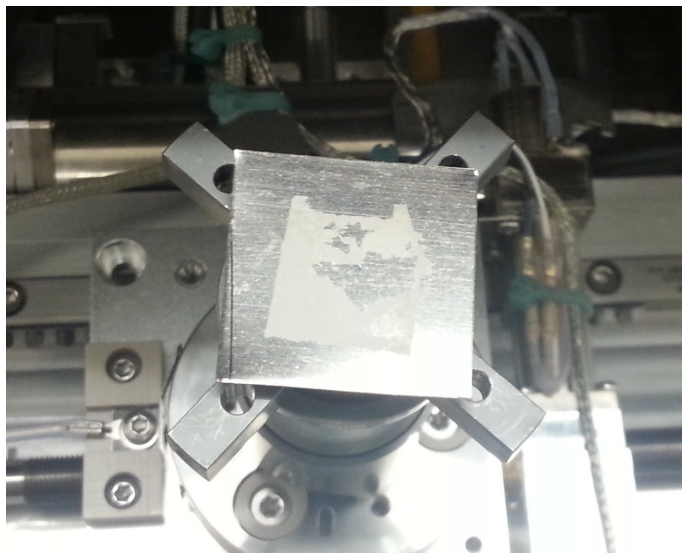


Figure 12: The deposit (opaque white region) on the platinum substrate. It is expected to be the nanowire.

- Copper and Sulfur: These two elements are expected to be the constituents of the nanowire. However, from EDX, it is not possible to know the ratio of Cu to S. We have to extract this information from another technique, for instance, XRD.
- Nitrogen and Carbon: These two elements are not expected to see, but this is not surprising. Since these are the basic ingredients of organic compounds in the environment around us. They are everywhere!
- Chlorine: This is not expected to detect either. Since the deposition is carried out in the solution containing HCl, it is also possible for chlorine to get incorporated in the nanowire. However, according to the growth mechanism mentioned in section 2.3, the chlorine atoms are not, in anyway, included in the nanostructure. It should, therefore, be concluded that the nanowire is not contaminated but coated by these chlorine.

In Figure 15, the brighter region implies the higher density of each element. As expected, copper, sulfur, and chlorine atoms gather around the area where the nanowire exists. For platinum, the area covered by the nanowire looks darker because the x-ray is blocked by it. Figure 15 also confirm that carbon and nitrogen are not the components of the structure, but rather be present everywhere.

4.4 Structure of nanowire

In order to find the stoichiometry of copper sulfide, we did x ray diffraction at P08 beam line at PETRA III. For the diffraction we used 25 keV x ray. The room temperature

x ray diffraction data is shown in Figure 16, which clearly confirms that our nanowires are Cu_2S . We have identified several peaks and comes to the conclusion that at room temperature copper sulfide is orthorhombic.

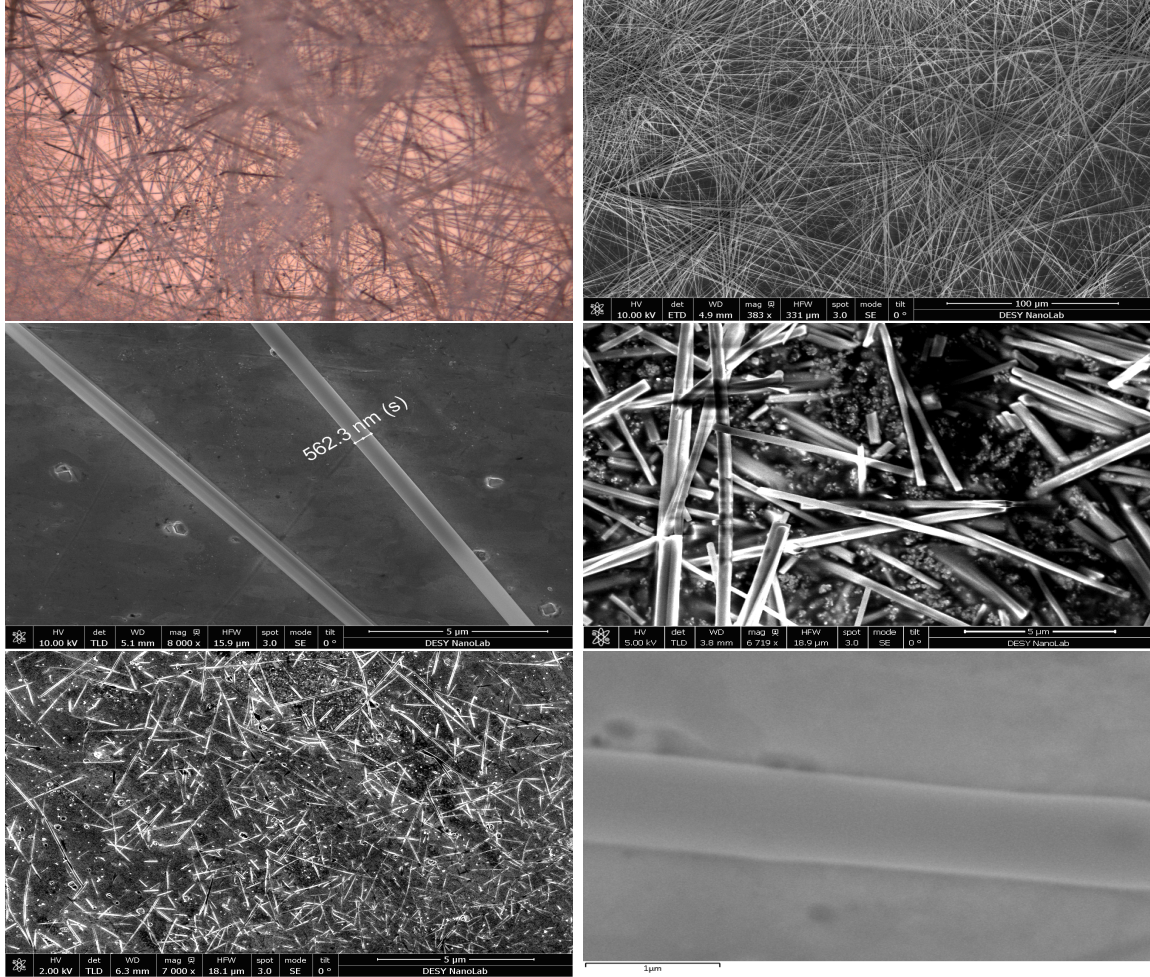


Figure 13: The images of nanowire seen under (a) an optical microscope and (b), (c), (d), (e), (f) electron microscopes. (b), (c), and (f) are the images of the same specimen but with different magnifying powers. (d), (e) are images of a specimens given from deposition with pH 1.2 and 1.6 of electrolyte, respectively.

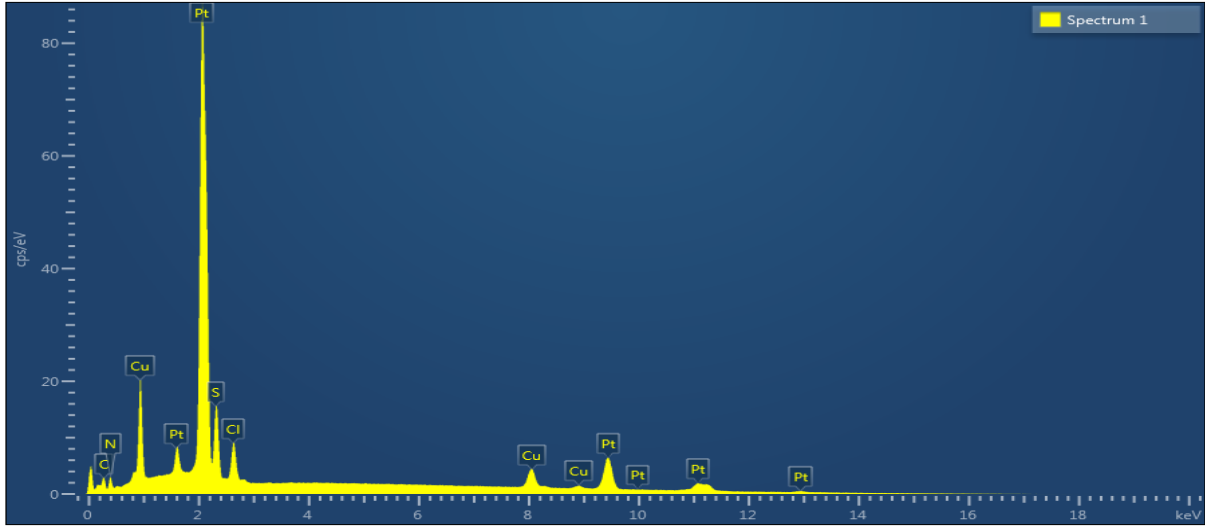


Figure 14: The energy-dispersive x-ray spectrum showing elemental components of the nanowire.

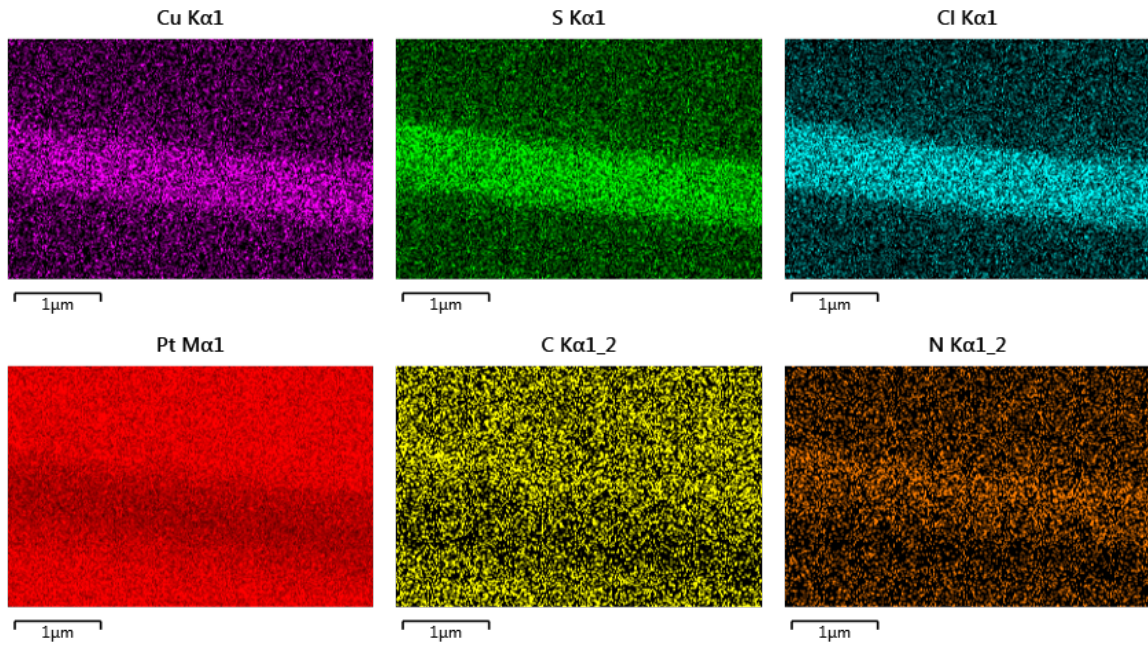


Figure 15: The elemental content of the nanowire in Figure 13(f). It is clearly seen that copper, sulfur, and chlorine are the components of the nanowire, whereas carbon and nitrogen are not.

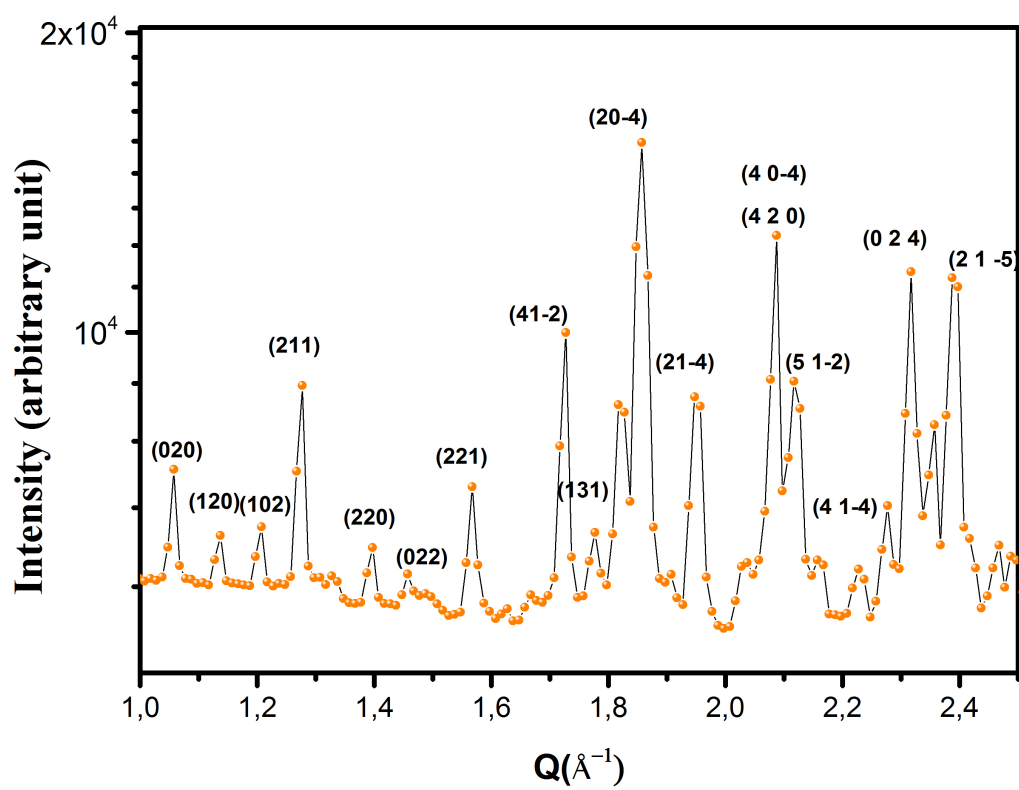


Figure 16: X ray diffraction spectrum

References

- [1] A. Ghahremaninezhad, E. Asselin, D. G. Dixon, *Electrodeposition and growth mechanism of copper sulfide nanowire*, J. Phys. Chem. C 2011, **115**, 9320-9334.
- [2] Takagi, M., *Electron-diffraction study of liquid-solid transition of thin metal films*, J. Phys. Soc. Jpn **9**, 359363 (1954).
- [3] Blackman, M. and Sambles, J. R., *Melting of very small particles during evaporation at constant temperature*, Nature **226**, 938938 (1970).
- [4] Couchman, P. R. and Jesser, W. A., *Thermodynamic theory of size dependence of melting temperature in metals*, Nature **269**, 481483 (1977).
- [5] Singh, V. N. and Mehta, B. R., *Nanoparticle size-dependent lowering of temperature for phase transition from $\text{In}(\text{OH})_3$ to In_2O_3* , J. Nanosci. Nanotechnol. **5**, 431435 (2005).
- [6] Hoshina, T., Kakemoto, H., Tsurumi, T., Wada, S. and Yashima, M., *Size and temperature induced phase transition behaviors of barium titanate nanoparticles*, Appl. Phys. Lett. **99**, 054311 (2006).
- [7] Chernyshova, I. V., Hochella, M. F. Jr and Madden, A. S., *Size-dependent structural transformations of hematite nanoparticles*, Phys. Chem. Chem. Phys. **9**, 17361750 (2007).
- [8] Guo, Y. G., Lee, J. S. and Maier, J., *AgI nanoplates with mesoscopic superionic conductivity at room temperature*, Adv. Mater. **17**, 28152819 (2005).
- [9] Guo, Y. G., Lee, J. S., Hu, Y. S. and Maier, J., *AgI nanoplates in unusual 7H/9R structures. Highly ionically conducting polytype heterostructures*, Electrochem. Soc. **154**, K51K60 (2007).